Enhanced precipitation of magnesium carbonates using carbonic anhydrase

Journal:	*Nanoscale*
Manuscript ID	NR-ART-06-2022-003199.R1
Article Type:	Paper
Date Submitted by the Author:	05-Aug-2022
Complete List of Authors:	Caulfield, Brian; Stevens Institute of Technology, Civil, Environmental and Ocean Abraham, Juliana; Stevens Institute of Technology, Civil, Environmental and Ocean Christodoulatos, Christos; Stevens Institute of Technology, Civil, Environmental and Ocean Prigiobbe, Valentina; Stevens Institute of Technology, Civil, Environmental and Ocean

Journal Name

ARTICLE TYPE

Cite this: DOI: 00.0000/xxxxxxxxxx

Enhanced precipitation of magnesium carbonates using carbonic anhydrase‡

Brian Caulfield,[a] Juliana Abraham,[a], Christos Christodoulatos[a], and Valentina Prigiobbe[a,*]

Received Date
Accepted Date

DOI: 00.0000/xxxxxxxxxx

Carbonate precipitation, as part of the carbon dioxide (CO_2) mineralization process, is generally regarded as a high-temperature, high-pressure, and high-purity CO_2 process. Typical conditions consist of temperatures around 120 °C and a pressure of 100 bar of pure CO_2, making the process costly. A major challenge facing carbonate precipitation is performing the reaction at low temperatures and low partial pressures of CO_2 (p_{CO2}) such as 25 °C and CO_2 flue gas concentration. In this work, we investigated the effect of carbonic anhydrase (CA) to favor magnesium (Mg) carbonate precipitation at low temperatures and low p_{CO2}. CA is an enzyme that accelerates CO_2 hydration promoting its conversion into HCO_3^- and then CO_3^{2-}. This increases supersaturation with respect to Mg-carbonates. A geochemical model was implemented and used to identify supersaturated conditions with respect to Mg-carbonates. Tests were run at 25, 40, and 50 °C and at 1 bar of either pure CO_2 or 10 vol.% CO_2 and 90 vol.% N_2. The concentration of 10 vol.% CO_2 was chosen to resemble CO_2 concentration in flue gas. In selected tests, the CA enzyme was added directly as bovine CA or through microalgae (*Scenedesmus obliquus*). Experiments were run for 48 hours; 24 hours to reach equilibrium, then another 24 hours until the supersaturated conditions were established. After 48 hours the experiments were interrupted and the solids were characterized. Results show that the addition of CA, either directly or through *Scenedesmus obliquus*, enhances Mg-carbonate precipitation. Regardless of the temperature, the precipitates were made entirely of nesquehonite ($MgCO_3$-$3H_2O$) when pure CO_2 was used. Otherwise, a solid solution containing brucite ($Mg(OH)_2$) and $MgCO_3$-$3H_2O$ was formed. Overall, these findings suggest that CA can promote carbonate precipitation at low temperatures, pressures, and CO_2 purity. The enzyme is effective when added directly or supplied through microalgae, opening up the possibility for a CO_2 mineralization process to be implemented directly at a combustion plant as a CO_2 storage option without preliminary CO_2 capture.

1 Introduction

The Paris agreement was created to ensure that the global average temperature does not raise more than 2 °C above pre-industrial levels[1]. Another facet of the agreement was focused on pursuing new technologies and methods to limit the temperature increase to 1.5 °C above pre-industrial levels[1]. The report of the Intergovernmental Panel on Climate Change (IPCC) concluded that in order to limit warming to 1.5 °C negative emissions technologies (NETs) must be implemented by the middle of this century[2]. A large portfolio of NETs are available; including coastal blue carbon, terrestrial carbon removal and sequestration, bioenergy with carbon capture and sequestration, direct air capture, geologic sequestration, and carbon dioxide (CO_2) mineralization (aka mineral carbonation).

CO_2 mineralization is an attractive NET solution because it has the potential to permanently sequester CO_2 into stable minerals without long-term monitoring and liability issues. Conventional CO_2 mineralization is an *ex situ* technology that relies on the dissolution of silicates (e.g., olivine, serpentinite, and wollastonite) within mafic and ultra-mafic rocks. This technology also relies on the precipitation of carbonates to fix carbon into stable carbonate crystals which can be reused in construction[3–5]. In contrast to the emerging alternative option of *in situ* CO_2 mineralization[6,7], *ex situ* CO_2 mineralization has the advantage of being an above-ground technology. Unlike *in situ* CO_2 mineralization, above-ground technology like *ex situ* CO_2 mineralization is beneficial because it can be monitored and controlled. However, the process typically relies on material pre-processing (grinding and milling), high temperatures, and high partial pressures of CO_2 (p_{CO_2})[8–11]. These conditions are strenuous, making the process

---

[a] *Department of Civil, Environmental, and Ocean Engineering, Stevens Institute of Technology, Hoboken (NJ), 07030, U.S.A.*
[*] *Corresponding author, E-mail: valentina.prigiobbe@stevens.edu*

† Electronic Supplementary Information (ESI) available as a pdf enclosed with this manuscript.

‡ Unclassified - Distribution A: Approved for Public Release; Distribution is Unlimited

costly[12].

To offset this cost several authors have proposed alternative sources of alkalinity, which are more reactive, such as industrial waste, mine tailing, and brines (including salt lake brines, mine drainage, seawater, and desalination brines)[13–18]. With these alternative sources CO_2 mineralization can be carried out at low temperatures and low p_{CO_2}. Brines are particularly interesting because alkaline earth elements (e.g., Ca, Mg, and Na) are readily accessible for precipitation. The accessibility of these elements means that neither rock pre-processing nor rock dissolution are required. Additionally, the concentrations of these elements can be significant, making lower temperatures and p_{CO_2} possible. However, the precipitation of stable carbonates (such as magnesite and calcite) at low temperatures still remains a challenge[19,20], and new approaches to catalyze the reaction are being investigated. For instance, the addition of carbonate seeds[21], organic additives (e.g., ferric EDTA)[22], polystyrene microspheres[23], microorganisms (such as microalgae)[24,25], and enzymes (such as carbonic anhydrase (CA))[25–27] have been proposed. Microalgae excrete extracellular CA which accelerates CO_2 hydration, promoting its conversion into HCO_3^- and CO_3^{2-} ions and favoring carbonate precipitation. Microalgae and cyanobacteria (e.g., *Scenedesmus obliquus*, *Chlorella vulgaris*, and *Anabaena variabilis*) produce CA naturally[28,29] through a carbon concentrating mechanism that allows them to grow fast at low p_{CO2} concentrations. In living organisms CA has been shown to be an integral component of biogenic Ca-carbonate formation[30]. As of yet, the effect of microalgae on carbonate precipitation from brines at low temperatures and low p_{CO_2} has not been studied.

In this paper, we present an experimental work on the precipitation of Mg-carbonates at low temperatures and p_{CO_2} in the presence of both bovine CA and *Scenedesmus obliquus*. Geochemical simulations were carried out to determine supersaturated conditions with respect to Mg-carbonates. Through systematic experiments with consistently varied conditions, we illustrate the mineralization of solid products characterized using X-ray diffraction and electron microscopy.

2 Materials and Methods

2.1 Set-up

Precipitation experiments were carried out with a continuously stirred batch reactor (Series 5100 Glass Reactor, Parr Instrument, U.S.A.), which we employed in an earlier paper[31] and upgraded for this work. A schematic of the set-up is shown in Figure 1 and a photo is reported in Figure 1 of the Supporting Information (SI) document. The reactor consists of a double-jacket glass vessel connected to a cylinder of CO_2 (99.99% purity, Welding Supply Company, U.S.A.) and a temperature controlling system (HE Heating Circulator, Julabo, U.S.A.). During each experiment the temperature and pressure were continuously measured and digitally recorded with online sensors (Parr 4848 Reactor Controller, Parr Instrument Company, U.S.A.) placed inside the reactor. A high-pressure pipette (Parr Liquid Charging Pipette, Parr Instrument Company, U.S.A.) was used to inject a solution into the vessel after stabilization (explained more in detail in section 2.2). The pipette was filled with a solution of given composition and pressurized with nitrogen gas (N_2, 99.99% purity, Welding Supply. U.S.A.). The pipette was pressurized at a slightly higher pressure than that in the reactor in order to overcome the resistance of the CO_2 rich atmosphere (approximately 1 bar).

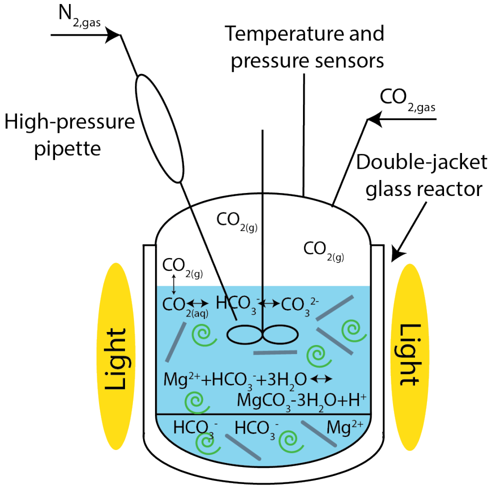

Fig. 1 Schematic of the set-up used for the experiments in this work. The light was used in the presence of microalgae.

2.2 Experiments

Precipitation experiments were carried out using the set-up described in section 2.1. First, a 400 mL solution was prepared using ultrapurified water (Milli-Q, U.S.A.) and sodium hydroxide (NaOH, 98.9% purity, Sigma-Aldrich) at a concentration of 1.5 molar. Then, the reactor was stabilized for 24 hours at a temperature and CO_2 partial pressure chosen on the basis of the operating conditions to be tested while stirring at a medium speed. The total pressure inside the reactor was always set equal to 1 ± 0.2 bar, but the partial pressure of CO_2 changed between 1 and 0.1 bar. This was established by using a cylinder of simulated flue gas or pure CO_2. In the cylinder with simulated flue gas, the chemical make-up was 10 vol.% CO_2 and 90 vol.% N_2. Additives were used in some experiments and they were placed into the initial NaOH solution. The additives were either pure bovine CA or microalgae (*Scenedesmus obliquus*). The concentrations of the additives were varied throughout the experiments. The activity of the CA was measured before and after the stabilization phase. After the initial solution was in the reactor for 24 hours, a 30 mL solution prepared using ultrapurified water and magnesium chloride ($MgCl_2 \cdot 6H_2O$, Sigma-Aldrich) at a concentration between 0.5 and 3 molar $MgCl_2 \cdot 6H_2O$ was injected into the reactor using the high-pressure pipette. The composition of the solution (concentration of Na and Mg) was selected to represent a deep surface brine as an alternative to the conventional approach in CO_2 mineralization based on mafic/ultramafic rock dissolution.

After this injection, the mixture was maintained at the selected temperature and pressure conditions for 24 hours. Upon completion, the stirring was stopped while the reactor depressurized. The solids were allowed to settle, and then were collected via filtration. Before characterization the solids were dried at room temperature and pressure conditions. In two experiments, namely exp. 26 and 27 (reported in Table 1 below), the time was altered to observe how the time affected the results. During the experiments where freshwater microalgae was added to the system, the reactor was continuously illuminated by 4 LED lights (40 W, 36 LED, 25 cm in length and 2 cm in width). These lights were equally distributed around the vessel (Figure 1) to achieve 98 μmol/(m^{2}s) of LED light intensity. The rationale behind the lighting is to maintain microalgae activity and promote the excretion of CA from the cells into the solution.

2.3 Selected enzyme and microorganism

The additives consist of pure lyophilized powder enzyme CA from bovine erythrocytes (Sigma-Aldrich. U.S.A.) and freshwater green microalga (*Scenedesmus obliquus* ATCC® 11477) (Figure 2). Pure CA was added directly to the initial solution. A microalga culture was grown for 7 days in a growth chamber at 25 °C and under continuous shaking at 120 rpm. The growth medium used was BG-11, whose recipe is described in an earlier paper[31]. The culture was centrifuged and the pellet washed with ultrapurified water 5 times before the cells were added into the NaOH solution. This washing process removes all nutrients from the supernatant growth medium and avoid possible interference in the mineralization process.

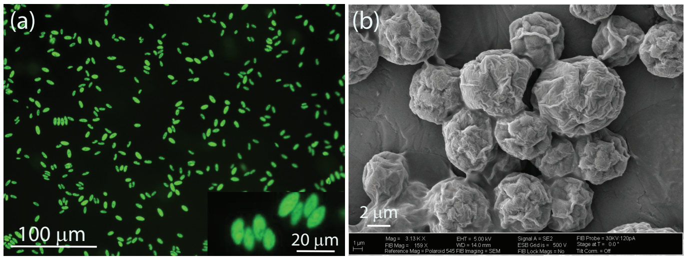

Fig. 2 *Scenedesmus obliquus* images performed using: (a) fluorescence microscopy; and (b) electroscanning microscopy.

2.4 Characterization of the additives

The tested concentrations for these additives (c_{add}) ranged from 0.14 to 0.40 g/L for *Scenedesmus obliquus* and 0.035 to 0.2 g/L for CA. The pure CA values were chosen according to Power *et al.*[27] and Fuchs *et al.*[32] while *Scenedesmus obliquus* values were increased incrementally. The total suspended solids and the enzymatic activity of the culture was calculated for each experiments using microorganisms. Enzymatic activity of pure CA as well as from microalgae was assayed spectrophotometrically using a method adapted for determining p-nitrophenyl acetate (p-NPA) activity[33]. Briefly, this assay is based on the enzyme mediated hydrolysis of p-NPA. CA has the same active site for the hydration reaction of CO_2 as that for the hydrolysis reaction of p-NPA. The latter reaction is much slower than the former, making it suitable for CA activity determination. P-NPA is hydrolyzed by the esterase activity of CA and the product of bright-yellow color can be spectrophotometrically determined by analyzing the absorbance at 400 nm.

2.5 Characterization of the solid products

The solids were characterized by scanning electron microscope (SEM, Auriga 40, Zeiss) and X-ray diffraction analysis (XRD, Ultima IV, Rigaku). The XRD measurements of our products were compared with reference spectra of carbonates[34].

3 Geochemical model

The open-source software PHREEQC.5[35] with the Pitzer database was used to determine the chemical composition of the system and design the experiments. The chemical reactions for the precipitation of the magnesium carbonate minerals such as artinite ($\mathrm{Mg_2(CO_3)(H_2O)\cdot 3}H_2\mathrm{O}$), nesquehonite ($\mathrm{MgCO_3\cdot 3H_2O}$), hydromagnesite ($\mathrm{Mg_5(CO_3)4(OH)_2\cdot 4H_2O}$), and magnesite ($\mathrm{MgCO_3}$) are, respectively,

$$\mathrm{Mg_2(CO_3)(OH)_2\cdot 3H_2O_s + 3H^+ \longleftrightarrow 2Mg^{2+} + HCO_3^- + 5H_2O}, \quad (1)$$

$$\mathrm{MgCO_3\cdot 3H_2O_s + H^+ \longleftrightarrow Mg^{2+} + HCO_3^- + 3H_2O}, \quad (2)$$

$$\mathrm{Mg_5(CO_3)_4(OH)_2\cdot 4H_2O_s + 6H^+ \longleftrightarrow 5Mg^{2+} + 4HCO_3^- + 6H_2O}, \quad (3)$$

$$\mathrm{MgCO_{3,s} + H^+ \longleftrightarrow Mg^{2+} + HCO_3^-}, \quad (4)$$

and the dominant reactions (i.e., the compounds have a concentration larger than 10^{-6} m) of the aqueous speciation are,

$$\mathrm{Mg(OH)_{2,a} \longleftrightarrow Mg^{2+} + 2OH^-}, \quad (5)$$

$$\mathrm{CO_{2,g} \longleftrightarrow CO_{2,a}}, \quad (6)$$

$$\mathrm{CO_{2,a} + H_2O \longleftrightarrow H_2CO_3}, \quad (7)$$

$$\mathrm{H_2CO_3 \longleftrightarrow HCO_3^- + H^+}, \quad (8)$$

$$\mathrm{HCO_3^- \longleftrightarrow CO_3^{2-} + H^+}. \quad (9)$$

Composition diagrams were created at 25 and 40 °C and $p_{\mathrm{CO_2}}$ of 1 and 0.1 bar by running PHREEQC from MATLAB[36] through the IPhreeqc module. The diagrams are reported as a function of Na^+ and Mg^{2+} concentrations in Figures 3 and 4. They show the contours of pH and saturation indexes (*SI*) with respect to magnesium carbonate minerals, whose reactions are given in eqn. 1 through 4,

$$SI_{art} = \mathrm{Log}\left(\frac{a^2_{Mg^{2+}} a_{HCO_3^-} a^5_{H_2O}}{a^3_{H^+} K_{sp,art}}\right), \quad (10)$$

$$SI_{nes} = \mathrm{Log}\left(\frac{a_{Mg^{2+}} a_{HCO_3^-} a^3_{H_2O}}{a_{H^+} K_{sp,nes}}\right), \quad (11)$$

$$SI_{hyd} = \mathrm{Log}\left(\frac{a^5_{Mg^{2+}} a^4_{HCO_3^-} a^6_{H_2O}}{a^6_{H^+} K_{sp,hyd}}\right), \quad (12)$$

$$SI_{mag} = \mathrm{Log}\left(\frac{a_{Mg^{2+}} a_{HCO_3^-}}{a_{H^+} K_{sp,mag}}\right), \quad (13)$$

where a and K_{sp} are the activities and the solubility products of the subscript species and solid phases, respectively. In all cases, the system is undersaturated with respect to $MgOH_2$ as it is possible to see in Figure 2 in the SI document.

4 Results and discussion

In this section, the results of this work are presented and discussed. Table 1 lists the operating conditions applied during the experiments together with the type of solid products obtained and the total mass of the solids determined after washing and drying at room conditions. In Figure 5, the temperature and pressure profiles recorded during two representative experiments are presented. As it is clear to see in the graph, the pressure is temporarily affected by solution injection with the high-pressure pipette but it re-establishes around the set value of 1 bar soon afterwards. The temperature is not affected by the injection or the precipitation reaction. This is the case for all the experiments.

4.1 Tests run at 25 °C

In this section, the mineralogical phases and morphologies of the products obtained at the end of the experiments performed at 25 °C are reported and discussed. In these tests the partial pressure of CO_2 was set equal to either 1 bar of pure CO_2 or 0.1 bar of CO_2 flue gas concentration. The tests were run with no additives, by adding microalgae, or by adding bovine CA to the system. No precipitation was observed in exp. 1 through 4 (no additves, 1 bar pure CO_2) despite the supersaturated conditions (see Figure 3 panels a through d) with respect to the hydrated metastable phase of $MgCO_3{\cdot}3H_2O$. Previous works show precipitation at similar conditions[31,37]. However, in those cases the reactor was slightly depressurized in order to inject the solution containing Mg^{2+}. Depressurization, even for a few seconds, temporarily reduces the CO_2 concentration in the atmosphere leading to an increase in pH that may favor precipitation. Degassing of CO_2 has even been used in earlier works to favor $MgCO_3{\cdot}3H_2O$ precipitation[25]. In our work, we used a high-pressure pipette that allowed us to avoid depressurization of the reactor and disturbance to the aqueous system.

No experiments were run at 25 °C and 0.1 bar without additives because the system was undersaturated with respect to $MgCO_3{\cdot}3H_2O$ at those conditions (see Figure 3 panels e through h). When an additive was used at p_{CO_2} of 1 bar the experiments (exp. 16 to 14 in Table 1) consistently produced seemingly pure $MgCO_3{\cdot}3H_2O$, as shown in Figure 6. The temperatures of exp. 16 through 14 were slightly higher than 25 °C due to the lights used during the algae experiments. This increase was unintentional and small enough to be considered negligible. Since the only condition that significantly changed between exp. 1 through 4 and exp. 14 through 16 was the addition of algae, we can conclude that algae does aid in the formation of carbonate crystals and in the mineralization of CO_2.

Similar results were obtained when an additive was added at p_{CO_2} of 0.1 bar in exp. 19, 23, and 29 in Table 1. In the SEM-EDS and XRD analyses reported in Figure 7 it can be observed that a solid solution made of $Mg(OH)_2$ and Mg-carbonates formed. In all of the XRD analyses, an amorphous phase dominates in the product as indicated by the smooth bump between 20 and 40 2Θ. The peaks in the XRD analyses are characteristic of solids such as $Mg(OH)_2$, $MgCO_3{\cdot}3H_2O$, and $MgCO_3$. The geochemical simulations (Figure 2 in the SI document) indicate that the system is undersaturated with respect to $Mg(OH)_2$, however the addition of additives may change the solution composition, which is not considered in the simulation. This change favors the precipitation of $Mg(OH)_2$ as well as Mg-carbonate minerals. The precipitation of $Mg(OH)_2$ should be avoided as it competes with the desired products, the Mg-carbonate minerals. Though algae do help the experiment create a pure carbonate crystal at 1 bar, they lead to solid mixtures at 0.1 bar, as shown in Figure 7. It is important to point out that the EDS analysis of the solid product does not show any nitrogen on the surface, suggesting the additives are not in the precipitates.

Bovine CA was not tested at 1 bar of CO_2, it was only tested at 0.1 bar. It is however expected that bovine CA would have aided Mg-carbonate precipitation similarly to microalgae. As mentioned above, CA is an enzyme produced by microorganisms such as algae which favors the hydration of CO_2 increasing the concentration of HCO_3^- ions.

Inhibiting factors in these experiments could have been either temperature or p_{CO_2}. Higher temperature or p_{CO_2} may have limited $Mg(OH)_2$ precipitation and favor Mg-carbonate precipitation, instead. With this in mind, we ran tests at a higher temperature and the results are shown in section 4.2.

4.2 Tests run at 40 and 50 °C

In this section the experiments performed at temperatures of 40 and 50 °C are reported and discussed. Similarly to the section above, the partial pressure of CO_2 was set equal to either 1 bar or 0.1 bar. The tests were run with no additives, by adding microalgae, or by adding bovine CA to the system. In experiments run without additives, at 1 bar, and 40 °C (exp. 5 through 8, and 18 in Table 1) $MgCO_3{\cdot}3H_2O$ only precipitated in exp. 6 where the concentration of Mg^{2+} was 1.5 molar. In exp. 5 and 5R, despite the supersaturated conditions with respect Mg-carbonates, (see Figure 4) no solids formed. Figure 8 reports the SEM images and the XRD measurements of these experiments showing that the applied conditions were able to produce seemingly pure nesquehonite.

In exp. 17 the same conditions as exp. 6 were applied, except algae were added. The solid product that formed was $MgCO_3{\cdot}3H_2O$, as shown in Figure 9. The amount of product collected in exp. 17 was twice that collected at the end of exp. 6. This indicates that algae affect the rate at which the solid formed leading to double the amount of the solid in the same reaction time, namely 24 hours.

With the aim to investigate the effect of CO_2 partial pressure, p_{CO_2} was reduced to 0.1 bar. At 0.1 bar, the results show an amorphous phase within the solid products which may resemble $Mg(OH)_2$ (Figure 10). Even extending the precipitation reaction up to 8 days (exp. 27 In Table 1) no Mg-carbonate formed. In these tests, the solution was undersaturated with respect to $MgCO_3{\cdot}3H_2O$ (Figure 4 part f) suggesting that supersaturation with respect to $MgCO_3{\cdot}3H_2O$ is critical for the formation of Mg-

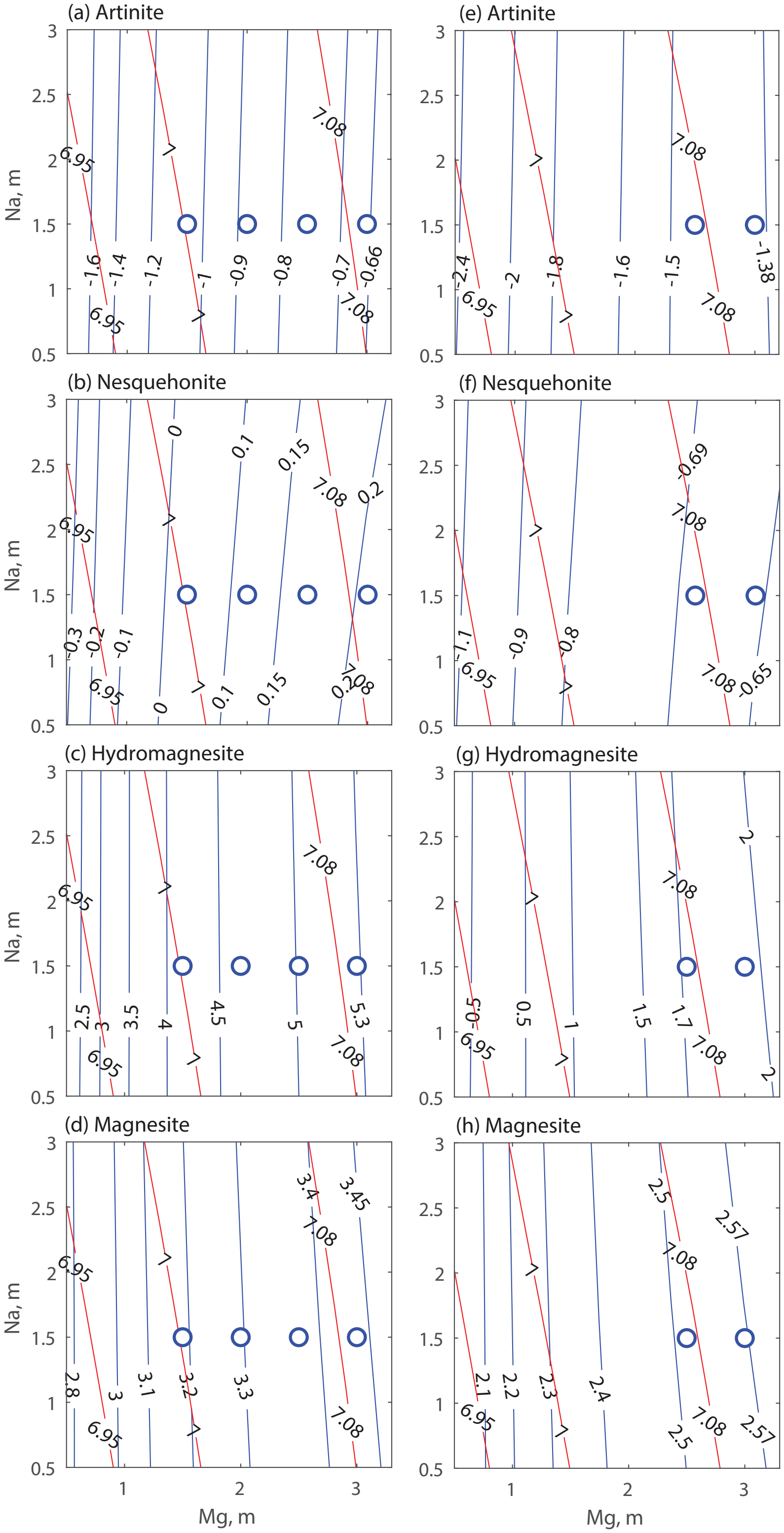

Fig. 3 Contours of pH (red) and *SI* (blue) calculated at 25 °C at p_{CO_2} equal to (a–d) 1 and (e–h) 0.1 bar. The dots indicate the applied experimental conditions.

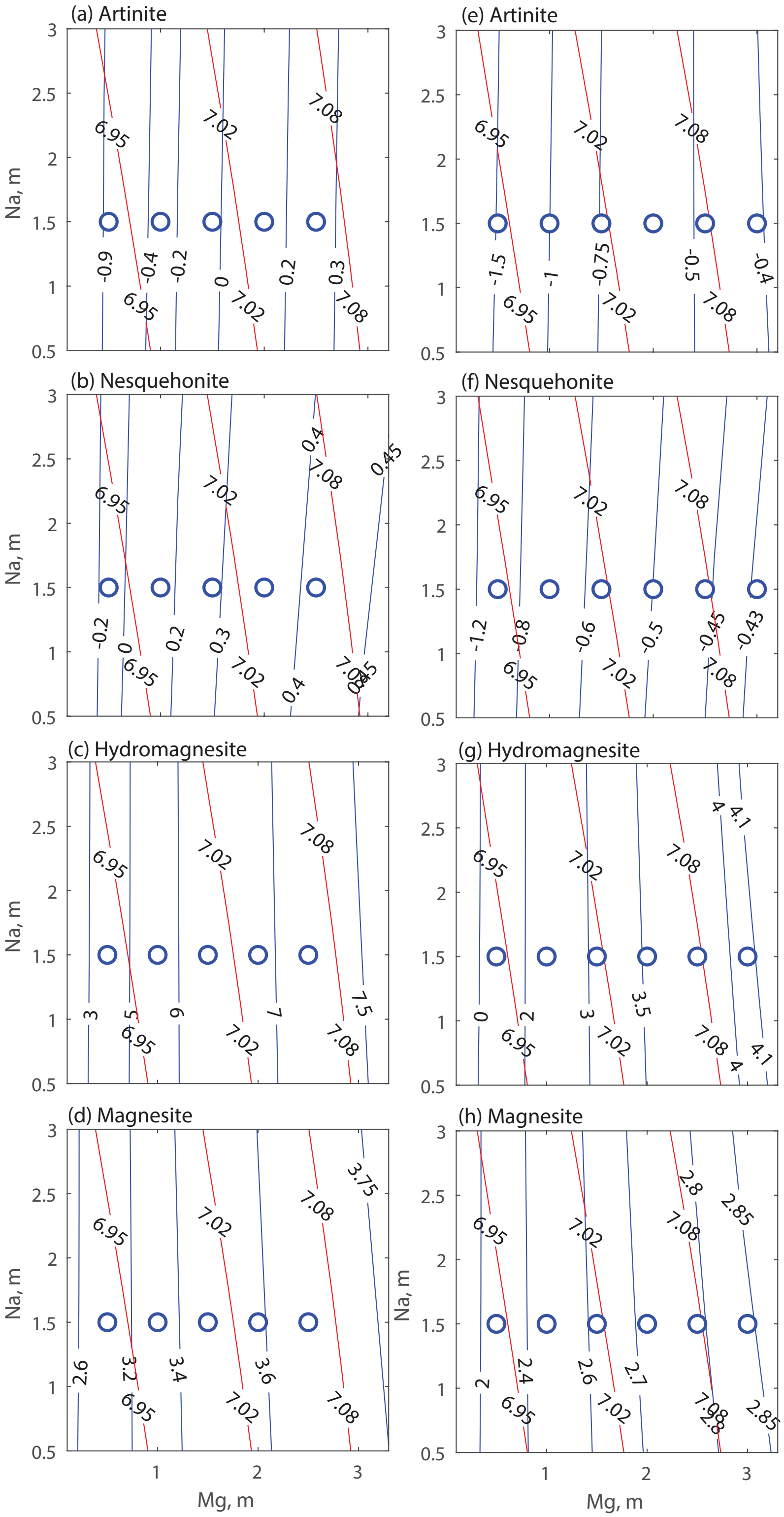

Fig. 4 Contours of pH (red) and *SI* (blue) calculated at 40 °C at $p_{\mathrm{CO_2}}$ equal to (a–d) 1 and (e–h) 0.1 bar. The dots indicate the applied experimental conditions.

Table 1 Operating conditions applied during the experiments and solid products. Symbols indicate: R#, repetition; †, 2 days of stabilization and 4 days of precipitation for a total of 144 hours; ‡, 1 day of stabilization and 8 days of precipitation for a total of 216 hours.

Exp.	T, °C	p_{CO_2}, bar	Na^+, mol/L	Mg^{2+}, mol/L	Type of additive	c_{add}, g/L	a_{CA}, u/L	Type of product	Product mass, g
1	25	1	1.5	1.5	-	-	-	-	-
2	25	1	1.5	2.0	-	-	-	-	-
3	25	1	1.5	2.5	-	-	-	-	-
4	25	1	1.5	3.0	-	-	-	-	-
16	27	1	1.5	2.0	Algae	0.20	171.9	Nesquehonite	3.87
15	28	1	1.5	2.5	Algae	0.20	165.4	Nesquehonite	2.09
14	29	1	1.5	3.0	Algae	0.21	170.3	Nesquehonite	8.91
14R	28	1	1.5	3.0	Algae	0.23	184.2	Nesquehonite	7.20
20	26	0.1	1.5	2.5	Algae	0.21	173.5	Brucite	19.7
19	27	0.1	1.5	3	Algae	0.14	26.4	Nesquehonite	22.6
19R1	25	0.1	1.5	3	Algae	0.14	145.3	Nesquehonite	20.3
19R2	25	0.1	1.5	3	Algae	0.22	149.7	Nesquehonite	21.7
19R3	25	0.1	1.5	3	Algae	0.21	153.5	Nesquehonite	22.4
19R4	25	0.1	1.5	3	Algae	0.40	354.1	Nesquehonite	20.6
23	25	0.1	1.5	3	Bovine CA	0.04	36.1	Nesquehonite	27.9
29	25	0.1	1.5	3	Bovine CA	0.10	112.7	Nesquehonite	25.3
18	40	1	1.5	0.5	-	-	-	-	-
5	40	1	1.5	1.0	-	-	-	-	-
5R	40	1	1.5	1.0	-	-	-	-	-
6	40	1	1.5	1.5	-	-	-	Nesquehonite	1.1
7	40	1	1.5	2.0	-	-	-	Nesquehonite	4.3
8	40	1	1.5	2.5	-	-	-	Nesquehonite	7.1
17	40	1	1.5	1.5	Algae	0.20	160.4	Nesquehonite	2.6
9	40	0.1	1.5	0.5	-		-	Brucite	1.2
9R	40	0.1	1.5	0.5	-	-	-	Brucite	1.6
10R	40	0.1	1.5	1.0	-	-	-	Brucite	6.5
11	40	0.1	1.5	1.5	-	-	-	Brucite	16.7
11R	40	0.1	1.5	1.5	-	-	-	Brucite	16.7
13R	40	0.1	1.5	2.5	-		-	Brucite	14.8
21	40	0.1	1.5	3.0	-	-		Brucite	15.4
26[†]	40	0.1	1.5	2.5	-	-	-	Brucite	12.1
27[‡]	40	0.1	1.5	2.5	-	-	-	Brucite	18.2
24	40	0.1	1.5	2.5	Bovine CA	0.04	36.1	Brucite	14.3
25	40	0.1	1.5	2.5	Algae	0.35	287.3	Nesquehonite	10.0
25R1	40	0.1	1.5	2.5	Algae	0.20	147.9	Nesquehonite	11.0
25R2	40	0.1	1.5	2.5	Algae	0.40	362.8	Nesquehonite	12.4

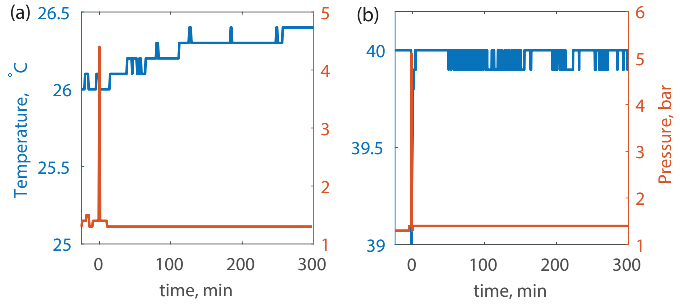

Fig. 5 Temperature and pressure measurements recorded during (a) exp. 20 and (b) exp. 13.

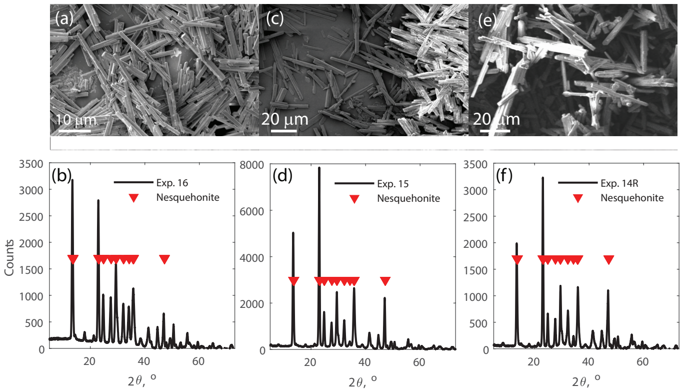

Fig. 6 Characterization of the solid products obtained from experiments (a–b) 16; (c–d) 15; and (e–f) 14 run at ∼25 °C and 1 bar of p_{CO_2} in the presence of microalgae *S. obliquus*.

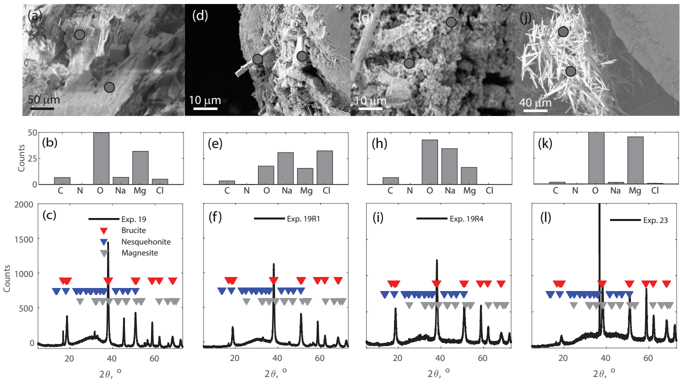

Fig. 7 Characterization of the solid products obtained from experiments (a–c) 19; (d–f) 19R1; (g–i) 19R4; and (j–l) 23 run at 25 °C and 0.1 bar of p_{CO_2} and in the presence of either microalgae *S. obliquus* or bovine CA as reported in Table 1.

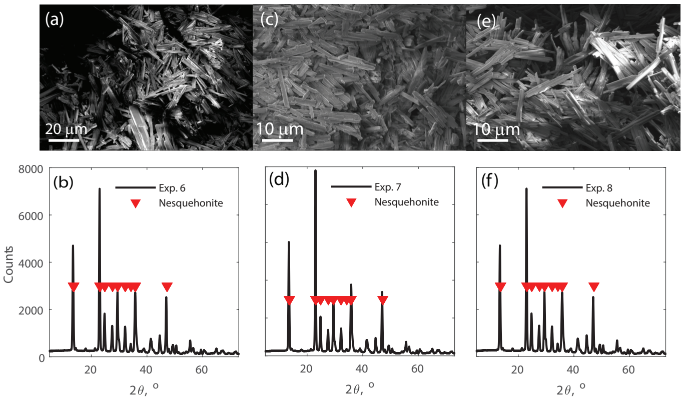

Fig. 8 Characterization of the solid products obtained from experiments (a-b) 6; (c-d) 7; and (e-f) 8 run at 40 °C and 1 bar of p_{CO_2}.

carbonates at these conditions.

Continuing tests at p_{CO_2} of 0.1 bar, additives were added to the solution (exp. 24 though 25R2). Exp. 24 did not yield carbonates, possibly due to the small concentration of the enzyme added. However, in the presence of algae, solids formed and they resembled a solid made of $Mg(OH)_2$, $MgCO_3{\cdot}3H_2O$, and $MgCO_3$ (Figure 11). Similar to the results at 25 °C, the EDS analyses of the solid products do not show any nitrogen, indicating no inclusions of additives in the precipitates. As the enzyme activity of microalgae was increased from 287.3 to 362.8 u/L, neither the amount nor the characteristics of the solid products changed.

The results from the experiments at 40 °C show that the precipitation reaction of Mg-carbonates is dependent on the p_{CO_2} and concentration of the enzyme. Increasing p_{CO_2} or enzyme concentration favor the precipitation of Mg-carbonates. But raising the temperature to 50 °C (exp. 28 in Table 1) did not favor precipitation. This is because solubility of CO_2 decreases with temperature lowering the supersaturation ratio values with respect to Mg-carbonates. The enzyme was not added at this temperature because of more rapid decay.

4.3 Stability of carbonic anhydrase during the experiments

We analyzed the stability of the enzyme for all experiments in which additives were used. The enzyme activity was measured at the beginning of the experiment, after the 24-hr stabilization period, and at the end of the experiment. The development of the activity over time is shown in Figure 12. In these diagrams, it is possible to see that during the stabilization period there is not significant change of the activity, although a slight decrease can be observed. This confirmed that the enzyme is stable during the 24-hr stabilization period, confirming that the determination of the enzyme activity at the beginning of a test is representative of that when the supersaturated conditions are established. However, after the precipitation reaction occurs, the activity decreases of 60–80%. The largest drop in CA activity corresponds to the largest initial CA in the system. There might be several reasons that explain this. Pure CA requires cold temperatures (around 4 °C) for storage in order to maintain its integrity. Since the experiments were run at higher temperatures (either 25 or 40 °C) CA might have undergone thermal degradation. If the temperature were the cause, then the CA should have degraded more at 40 °C than 25 °C. However, the trends of the activity in the two parts of Figure 12 are very similar. Alternatively, precipitation may have removed CA either through inclusion in the solid structure or sweeping. However, EDS analyses do not show any nitrogen element on the surface of the precipitates. A more likely explanation is that CA degrades over time. We ran preliminary tests to determine the correlation between total solid concentration and CA activity (Figure 3 SI document). In these tests, we

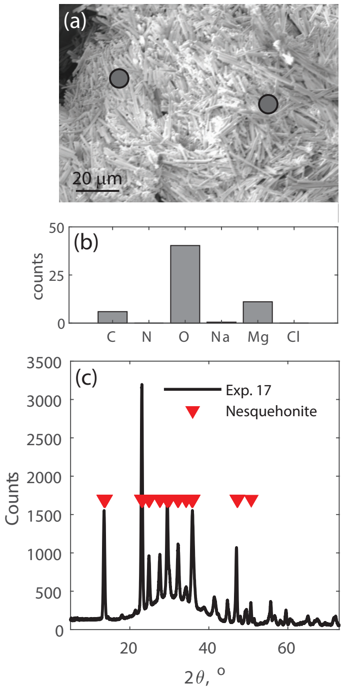

Fig. 9 Characterization of the solid product obtained from experiments 17 run at 40 °C and 1 bar of p_{CO_2} in the presence of algae.

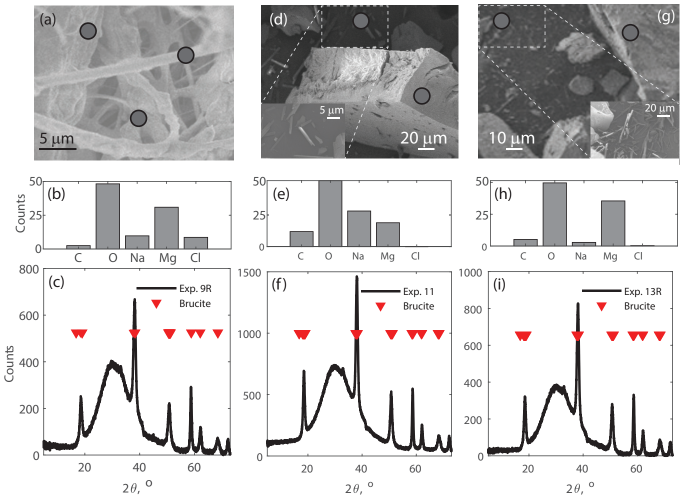

Fig. 10 Characterization of the solid products obtained from experiments (a–c) 9; (d–g) 11; and (h–i) 13R run at 40 °C and 0.1 bar of p_{CO_2}.

noticed that the same sample of pure CA 24 hours apart showed a significant reduction in CA activity. Given that the precipitation experiments were ran for 48 hours, the enzyme activity might have dropped. The combination of temperature, hydration, and decrease of pH upon precipitation may have accelerated this decay.

5 Conclusions

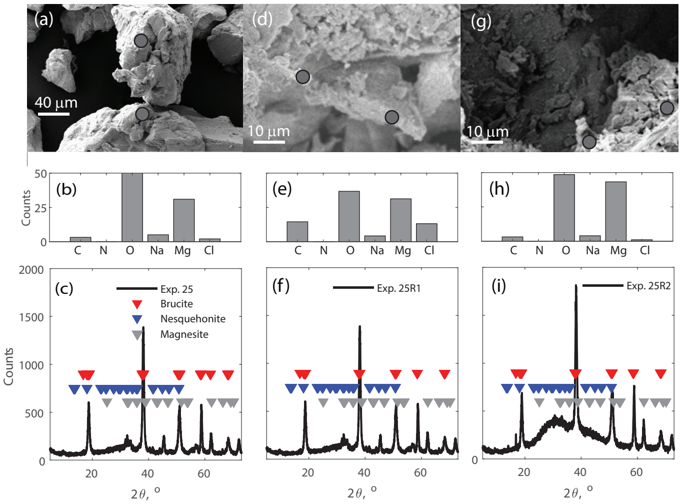

Fig. 11 Characterization of the solid products obtained from experiments (a–c) 25; (d–g) 25R1; and (h–i) 25R2 run at 40 °C and 0.1 bar of p_{CO_2} and in the presence of microalgae *S. obliquus* and bovine CA as reported in Table 1.

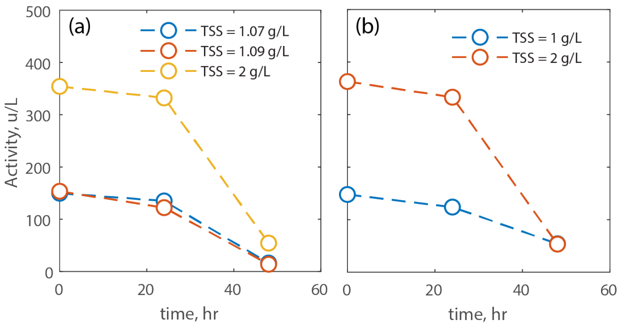

Fig. 12 Evolution of the activity of CA within the microalgae at (a) 25 °C and (b) 40 °C. CA was added to the system through different amount of microalgae expressed as total suspended solids (TSS).

In this paper, we present a study on the effect of temperature, partial pressure of CO_2 (p_{CO_2}), and carbonic anhydrase enzyme on Mg-carbonate precipitation. The enzyme was added directly as bovine CA or through microalgae (*Scenedesmus obliquus*). A geochemical model was implemented and used to select the operating laboratory conditions. Systematic tests at 25 and 40 °C and total pressure of 1 bar were run. The values of p_{CO_2} were varied between 1 and 0.1 bar to simulate pure CO_2 and flue gas. The results show that the addition of CA through microalgae is effective in promoting the precipitation of a hydrated Mg-carbonate (nesquehonite,$MgCO_3$-$3H_2O$). This is due to the effect of the enzyme in promoting the conversion of CO_2 into HCO_3^- and CO_3^{2-} which increases the supersaturation ratio with respect to carbonate solid phases. However, the activity of the enzyme seems to decrease during the experiment and further investigation on its decay is needed.

Overall, this study demonstrates that the microalgae *Scenedesmus obliquus* can be used to enhance the precipitation of a hydrated Mg-carbonate mineral from a brine at low temperature and flue gas partial pressure (p_{CO_2}). This opens up the possibility to implement the direct conversion of CO_2 into carbonate minerals as a negative emission technology (NET) at a combustion plant, without prior capture.

Author Contributions

Brian Caulfield: data curation, investigation, methodology, and writing – original draft. Juliana Abraham: data curation, investigation, methodology, writing – original draft, and supervision. Christos Christodoulatos: Funding acquisition and writing – original draft. Valentina Prigiobbe: Conceptualization, data curation, formal analysis, funding acquisition, methodology, resources software, supervision, visualization, and writing – original draft.

Conflicts of interest

"There are no conflicts to declare".

Acknowledgements

This work was supported by the Industrial Base Resilience Initiative, sponsored by SIA Solutions LLC, US Army Corps of Engineers Mobile District under the prime contract No.: W91278-16-D-0007. The authors would like to thank four undergraduate students at Stevens Institute of Technology that helped in the first part of this project in summer 2021: Louise Gottwald, Stephanie Searing, and Hayley Kirmaier as part of the Pinnacle Scholar Program and Vijay Persaud as part of the Clark Scholar Program. The authors would also like to thank the graduate student Paula Sacripanti for her help adapting the CA analytical technique. Finally, the authors would like to thank the anonymous reviewers that helped to improve the manuscript with their comments.

Notes and references

1 UNFCCC, 2015.

2 H. de Coninck, A. Revi, M. Babiker, P. Bertoldi, M. Buckeridge, A. Cartwright, W. Dong, J. Ford, S. Fuss, J.-C. Hourcade, D. Ley, R. Mechler, P. Newman, A. Revokatova, S. Schultz, L. Steg and T. Sugiyama, *Strengthening and Implementing the Global Response. In: Global Warming of 1.5°C. An IPCC Special Report on the impacts of global warming of 1.5°C above pre-industrial levels and related global greenhouse gas emission pathways, in the context of strengthening the global response to the threat of climate change, sustainable development, and efforts to eradicate poverty Masson-Delmotte, V., P. Zhai, H.-O. Pörtner, D. Roberts, J. Skea, P.R. Shukla, A. Pirani, W. Moufouma-Okia, C. Péan, R. Pidcock, S. Connors, J.B.R. Matthews, Y. Chen, X. Zhou, M.I. Gomis, E. Lonnoy, T. Maycock, M. Tignor, and T. Waterfield (eds.)*, 2018.

3 B. Metz, O. Davidson, H. de Coninck, M. Loos and E. Meyer, L., *IPCC Special Report on Carbon Dioxide Capture and Storage; Intergovernmental Panel on Climate Change*, 2005.

4 M. Blondes, M. Merrill, S. Anderson, and C. DeVera, 2019.

5 S. Yadav and A. Mehra, *Environmental science and pollution research*, 2021, **28**, 12202–12231.

6 J. M. Matter and P. B. Kelemen, *Nature geoscience*, 2009, **2**, 837–841.

7 S. K. White, F. A. Spane, H. T. Schaef, Q. R. S. Miller, M. D. White, J. A. Horner and B. P. McGrail, *Environmental Science & Technology*, 2020, **54**, 14609–14616.

8 A. Sanna, M. Uibu, G. Caramanna, R. Kuusik and M. M. Maroto-Valer, *Chemical society reviews*, 2014, **43**, 8049–8080.

9 M. I. Rashid, E. Benhelal, F. Farhang, T. K. Oliver, M. S. Rayson, G. F. Brent, M. Stockenhuber and E. M. Kennedy, *Journal of cleaner production*, 2019, **212**, 151–161.

10 S. Hariharan and M. Mazzotti, *Chemical Engineering Journal*, 2017, **324**, 397–413.

11 G. Gadikota, J. Matter, P. Kelemen and A.-h. A. Park, *Physical chemistry chemical physics*, 2014, **16**, 4679–4693.

12 A. Kirchofer, A. Brandt, S. Krevor, V. Prigiobbe and J. Wilcox, *Energy & Environmental Science*, 2012, **5**, 8631–8641.

13 J.-H. Bang, Y. Yoo, S.-W. Lee, K. Song and S. Chae, *Minerals*, 2017, **7**, year.

14 J.-H. Bang, S. C. Chae, S.-W. Lee, J.-W. Kim, K. Song, J. Kim and W. Kim, *Journal of CO_2 Utilization*, 2019, **33**, 427–433.

15 C. M. Woodall, X. Lu, G. Dipple and J. Wilcox, *Minerals*, 2021, **11**, year.

16 I. M. Power, C. Paulo, H. Long, J. A. Lockhart, A. R. Stubbs, D. French and R. Caldwell, *Environmental Science & Technology*, 2021, **55**, 10056–10066.

17 Y. E. Chai, S. Chalouati, H. Fantucci and R. M. Santos, *Crystals*, 2021, **11**, year.

18 W. Liu, L. Teng, S. Rohani, Z. Qin, B. Zhao, C. C. Xu, S. Ren, Q. Liu and B. Liang, *Chemical Engineering Journal*, 2021, **416**, 129093.

19 V. Prigiobbe and M. Mazzotti, *Chemical Engineering Journal*, 2013, **223**, 755–763.

20 V. Prigiobbe, *Journal of Environmental Chemical Engineering*, 2018, **6**, 930–936.

21 S. Hariharan and M. Mazzotti, *Crystal Growth and Design*, 2016, **17**, 317–327.

22 G. Montes-Hernandez, M. Bah and F. Renard, *Journal of CO_2 Utilization*, 2020, **35**, 272–276.

23 I. M. Power, P. A. Kenward, G. M. Dipple and M. Raudsepp, *Crystal Growth & Design*, 2017, **17**, 5652–5659.

24 I. M. Power, S. A. Wilson, D. P. Small, G. M. Dipple, W. Wan and G. Southam, *Environmental Science & Technology*, 2011, **45**, 9061–9068.

25 T. K. Oliver, B. Z. Dlugogorski and E. M. Kennedy, *Minerals Engineering*, 2014, **61**, 113–120.

26 M. Zhang, L. Zhao, G. K. Li, C. Zhu, S. Dong, Z. Li, C. Tang, J. Ji and J. Chen, *Geomicrobiology Journal*, 2021, **38**, 549–560.

27 I. M. Power, A. L. Harrison, G. M. Dipple and G. Southam, *International Journal of Greenhouse Gas Control*, 2013, **16**, 145–155.

28 O. T. K. G. Madhumanti Mondal, Saumyakanti Khanra and G. Halder, *Environmental Progress Sustainable Energy*, 2016, **35**, 1605–1615.

29 J. da Costa Ores, M. C. A. D. Amarante, S. S. Fernandes and S. J. Kalil, *Biocatalysis and Biotransformation*, 2016, **34**, 57–65.

30 W. E. Müller, H. C. Schröder, U. Schlossmacher, M. Neufurth, W. Geurtsen, M. Korzhev and X. Wang, *FEBS Open Bio*, 2013, **3**, 357–362.

31 Z. Ye, J. Abraham, C. Christodoulatos and V. Prigiobbe, *Energy & Fuels*, 2019, **33**, 8843–8851.

32 W. Fuchs, F. Steger, J. Reich, D. Ribitsch, S. K.-M. Rittmann and G. Bochmann, *Catalysts*, 2021, **11**, 819.

33 Y. Pocker and J. T. Stone, *Biochemistry*, 1967, **6**, 668–678.

34 Y. H. S. N. Lafuente B, Downs R T, *Highlights in Mineralogical Crystallography, T Armbruster and R M Danisi, eds. Berlin, Germany, W. De Gruyter*, 2015, 1–30.

35 USGS, *PHREEQC (Version 3)–A Computer Program for Speciation, Batch-Reaction, One-Dimensional Transport, and Inverse Geochemical Calculations*, 2016.

36 MATLAB, *version (R2021a)*, The MathWorks Inc., Natick, Massachusetts, 2021.

37 M. Hänchen, V. Prigiobbe, R. Baciocchi and M. Mazzotti, *Chemical Engineering Science*, 2008, **63**, 1012–1028.